Journal of Constructional Steel Research 190 (2022) 107137

Contents lists available at ScienceDirect

Journal of Constructional Steel Research

journal homepage: www.elsevier.com/locate/jcsr

Influence of the imperfection direction on the ultimate response of steel frames in advanced analysis

Itsaso Arrayago [a,*], Kim J.R. Rasmussen [b]

[a] Universitat Politècnica de Catalunya, Dept. of Civil and Environmental Engineering, Spain
[b] The University of Sydney, School of Civil Engineering, Australia

ARTICLE INFO

Keywords:
Initial geometric imperfections
Advanced analysis
Elastic buckling analysis
Steel frames
Stainless steel frames

ABSTRACT

Initial geometric imperfections are unavoidable in steel members and frames due to erection and manufacturing tolerances. These include frame out-of-plumbness, member out-of-straightness and cross-sectional imperfections, and can have a significant influence on the response and resistance of steel structures. Thus, they need to be accounted for in the analysis and design of steel structures, especially when advanced design procedures are adopted. One of the easiest approaches to introduce geometric imperfections in structural finite element models is through the linear superposition of scaled eigenmodes, which are obtained from a priori elastic buckling analysis. Although the shape and magnitude of frame and member imperfections are specified in international standards, the rules for the combination of different types and directions of imperfections are unclear or impractical, and often require designers to consider many possible combinations to find the critical, or "worst case", shape of the imperfection including the direction of each eigenmode. This paper investigates the influence of the direction of modes contributing to the imperfection on the ultimate load (i.e., resistance) of steel frames when using advanced analysis. Ultimate loads are estimated from advanced finite element simulations for 20 regular and irregular unbraced frames featuring steel and austenitic stainless steel compact sections, in which initial imperfections are modelled as linear superpositions of six scaled buckling modes considering all possible combinations of direction. The results show that the influence of the imperfection direction on the ultimate frame load is small, and that assuming a combination of all buckling modes with positive amplitudes provides a simple and accurate estimation of the critical imperfection combination.

1. Introduction

Initial geometric imperfections can have a significant influence on the resistance and stiffness of steel frames, including frame out-of-plumbness imperfections, member out-of-straightness imperfections and local cross-sectional imperfections. Traditionally, the effect of sway imperfections has been accounted for in structural analyses by directly modelling the out-of-plumbness or through the use of equivalent notional horizontal loads, while member and cross-section imperfections have been implicitly considered in design expressions (e.g., the effect of member imperfections is incorporated in member strength design curves, and local imperfections in local buckling expressions). However, with the development and incorporation of direct design approaches in the current versions of international standards such as AISC 360 [1], AISC 370 [2], prEN 1993-1-14 [3], AS/NZS 4100 [4] and AS/NZS 4600 [5], a different and more detailed definition of initial geometric imperfections is required. In these direct design approaches, the resistance of the structure is directly evaluated from the analysis without requiring further resistance checks, and thus the incorporation of appropriate initial imperfections in the developed advanced finite element (FE) models is critical.

The most common approaches to consider the effects of initial geometric imperfections in advanced analysis are the modelling of imperfections by directly offsetting the coordinates of the nodes, the reduction of member stiffness, the adoption of notional horizontal forces and the superposition of scaled elastic buckling modes [6]. While the first approach is not practical for everyday engineering practice, one of the advantages of the stiffness reduction method is that it does not require an explicit modelling of the imperfections. Although several stiffness-reduction factors have been proposed to account for the effect of initial geometric imperfections [7–9], they have not been assessed through probabilistic approaches. The notional horizontal force method

* Corresponding author at: Jordi Girona 1-3, Building C1, 08034 Barcelona, Spain.
E-mail address: itsaso.arrayago@upc.edu (I. Arrayago).

https://doi.org/10.1016/j.jcsr.2022.107137
Received 20 July 2021; Received in revised form 4 January 2022; Accepted 6 January 2022
Available online 29 January 2022

has been widely adopted in different structural standards [1–5,10] for its simplicity, since it allows modelling structures in their theoretically perfect configuration and taking into account the effect of frame and member imperfections by introducing a set of equivalent horizontal forces. Typically, the elastic buckling mode approach assumes that the first eigenmode represents the most critical imperfection and it is scaled and introduced as the initial imperfection of the structure [10]. However, the actual failure mode of the structure may be different from the first buckling mode due to the significant plastic deformations and load redistribution occurring in advanced analysis. In this case, failure may occur in parts of the structure deficiently represented in the first buckling mode and hence, to ensure imperfections are introduced in all members, it is recommendable to include additional higher order eigenmodes when incorporating initial geometric imperfections [11]. Although the amplitude and the shape or pattern of each initial imperfection type are prescribed in specifications, and the different alternatives discussed above exist to input the imperfections in finite element models, standards usually require that the most critical combination of imperfection directions resulting in the minimum resistance be adopted as the nominal resistance of the structure. This is generally not practical, since the number of possible imperfection combinations is significant even for relatively simple frames. Furthermore, it can be argued that the treatment of initial imperfections may be different in the context of the traditional two-step design methods and for system-based direct design approaches.

In the traditional two-step design methodology, the prevailing analysis type for determining internal actions is the geometric nonlinear analysis (GNA), which elastically amplifies deformations caused by applied loads and frame out-of-plumbness imperfections, while member out-of-straightness imperfections and local cross-sectional imperfections are not modelled. In rigid and semi-rigid construction, moments are transferred through connections whereby vertical and inclined members are invariably subjected to both compression and bending, and hence need to be designed for combined loading. This is typically done using interaction equations, the simplest form of which is linear (Eq. (1)), and which are generally conservative.

$$\frac{N_{GNA}}{\phi_c N_m}+\frac{M_{GNA}}{\phi_b M_m}=1 \tag{1}$$

where (N_{GNA}, M_{GNA}) are the internal actions predicted by GNA analysis and (N_m, M_m) and (ϕ_c, ϕ_b) are the nominal member resistances and the resistance factors for compression and bending, respectively. In the Eurocode terminology, the interaction equation becomes Eq. (2), in which ($N_{b,Rk}$, $M_{b,Rk}$) are the characteristic member resistances for compression and bending and γ_{M1} is the partial safety factor for instability.

$$\frac{N_{GNA}}{N_{b,Rk}/\gamma_{M1}}+\frac{M_{GNA}}{M_{b,Rk}/\gamma_{M1}}=1 \tag{2}$$

The member capacities (N_m, M_m) or ($N_{b,Rk}$, $M_{b,Rk}$) are calculated using strength curves derived from tests and advanced numerical analyses based on a target value of member out-of-straightness, e.g., $L/1000$, where L is the member length. The ultimate capacity of the frame is deemed to be reached when the first (critical) member reaches its capacity, i.e., Eq. (1) or Eq. (2) are satisfied. The strength curves for calculating the member resistances are typically chosen to produce the mean or characteristic value of resistance when averaged over a length range, the reference being the target out-of-straightness chosen for the tests and advanced analysis. The resistance factors and the partial safety factor are calibrated such that the probability of the internal actions exceeding their respective member design capacity (e.g., $N_{GNA} > \phi_c N_m$) does not exceed a target value, typically expressed as a target reliability index (β_m). The calculation of these factors depends on the bias and variance of the strength curves relative to the "true" experimental and numerical resistances, which refer to the reference value of out-of-straightness.

In this procedure, it is implicitly assumed that the actual out-of-straightness imperfection of the critical member first reaching its capacity equals the target value, typically the tolerance value. The probability that this is the case is small as the imperfection of structural members very rarely reaches the tolerance value. A statistically more consistent approach would be to use the mean value of out-of-straightness, e.g., $L/1490$ as reported by Bjorhovde [12], or an updated mean value based on more recent data, e.g., $L/1996$ [13], since the mean value represents the most likely value of imperfection of any member, including the critical. The variance of the actual value of out-of-straightness of the critical member relative to the mean value is accounted for by considering the coefficient of variation of the design value relative to the test or "true" resistance in the reliability calibration.

It is evident that if higher strength curves based on a smaller target value of out-of-straightness are used for determining member resistances, and assuming the resistance of real specimens featuring random imperfection amplitudes represents the "true" resistance of the members, the resistance factors (ϕ_c, ϕ_b) would reduce if the target reliability index (β_m) is unchanged because the resistance reserve due to the conservatism of the strength curve would reduce. On the contrary, the partial safety factors (γ_{M1}) would increase under the same circumstances. Alternatively, if the resistance or partial safety factors are unchanged, the reliability index would reduce. These relationships emphasise the intrinsic interdependency between the chosen target out-of-straightness and the calculated reliability index.

Summarising this discussion of the traditional two-step design methodology,

1. the structure is assumed to fail when the first (critical) member reaches its capacity,
2. it is implicitly assumed that the out-of-straightness of the critical member equals the target value,
3. the target value of out-of-straightness is usually chosen as a tolerance value, whereas a statistically sound approach would be to choose the mean value of out-of-straightness,
4. the amplification of moments is underestimated when GNA analysis is used to calculate internal actions, and
5. the resistance of members subject to combined compression and bending is calculated using interaction curves which are typically conservative.

The calculation of resistance and partial safety factors to a target reliability index (β_m) is subject to these assumptions and inaccuracies.

The system-based direct design approaches are considerably more statistically consistent in their calculation of system resistance and partial safety factors [14,15]. The calibration uses accurate statistical functions obtained from field measurements (e.g., [11,16–18]) to represent all main random variables including out-of-straightness [17–20]. Monte-Carlo type simulations are performed considering the variance of all random variables in computing the probability of failure, which may be expressed in terms of the system reliability index (β_s), and the system resistance factor (ϕ_s) or the system partial safety factor ($\gamma_{M,s}$) are chosen so that the system reliability index meets or exceeds the target value. The direct design allows additional loading past the failure of the first critical members when load redistribution is possible until the complete failure of the frame. In this framework, the shape of the imperfection is chosen to produce resistances statistically consistent with the resistance of frames with measured shapes of imperfection [11]. In particular, the mean value of amplitude of out-of-straightness is the mean measured value, typically less than the tolerance value.

Direct design approaches require a nominal model be specified, including nominal values of material properties, geometric imperfections, residual stresses, etc. The choice of nominal geometric imperfection is largely arbitrary as the influence of the particular choice of nominal imperfection is reflected in the reliability calibration which

produces the system ϕ_s or $\gamma_{M,s}$ factors. It is possible, in the framework of system-based direct design, to adopt the more restrictive approach of determining the nominal resistance as the minimum resistance, which allows specifying less conservative values of ϕ_s and $\gamma_{M,s}$. Or conversely, it is also possible to accept a more permissive combination of initial imperfections and to prescribe the associated more conservative system factors.

Because system resistance and ϕ_s, $\gamma_{M,s}$-factors are now being calibrated for inclusion in international standards for the first time, it is timely for national standardisation committees to decide how initial imperfections should be treated in the determination of system nominal resistances and to prescribe system factors accordingly. In this consideration, it follows from the above discussion that the reliability indices obtained from the traditional two-step design methodology and system-based direct design approaches are not directly comparable. Seeing that the two-step design methodology ignores the potential additional capacity of the frame achievable by load redistribution in statically redundant frames after the critical member reaches its capacity, the system target reliability index should be chosen to be at least that of members for the two-step design methodology. Equally, if the frame is statically determinate, or failure occurs in a statically determinate part of a redundant frame, no load redistribution is possible and the target reliability of the two approaches should be equal, notwithstanding the inaccuracies associated with the member-based approach summarized above.

With the aim of simplifying the definition of initial imperfections in design, this paper investigates the influence of the direction of initial imperfections modelled as linear superpositions of buckling modes on the resistance of steel and stainless steel frames designed using advanced analysis. Section 2 provides an overview of the methodologies adopted in current structural standards for modelling initial imperfections and presents the alternative approach based on the superposition of buckling modes proposed in [11]. In Section 3, the benchmark frames used in the assessment are presented and the developed advanced finite element models are described. Finally, Section 4 presents the analysis of the variability in the resistances for different combinations of imperfection directions, and proposes a simple approach to modelling geometric imperfections without performing multiple analyses.

2. Modelling of initial geometric imperfections

2.1. Initial geometric imperfections in standards

Most major international design standards for steel structures prescribe design values for the different types of imperfections and specify how to include them in structural analyses, being rather consistent among the different standards. The definition of nominal initial geometric imperfections differs depending on the considered design method: in general, the consideration of frame out-of-plumbness (sway) imperfections is always required, while member imperfections only need to be included when advanced analyses are carried out.

The AISC 360 [1] and AISC 370 [2] Specifications require that out-of-plumbness imperfections corresponding to a nominal initial storey out-of-plumb angle ϕ of 1/500 be included when the Direct Analysis Method is adopted by directly modifying the position of the nodes or through the use notional loads, although the explicit modelling of initial out-of-straightness of individual members is not necessary since these imperfections are accounted for in the design provisions for compression members. Conversely, the analysis shall include the effects of system imperfections (with amplitudes of ϕ=1/500) and member imperfections (with amplitudes of L/1000) when the advanced analysis provisions given in Appendix 1 are adopted, and the use of notional loads to represent either type of imperfection is not permitted. Since advanced analysis provisions in [1,2] are currently limited to compact sections, it is not necessary to include cross-sectional imperfections in the FE model.

Regarding global sway imperfections, prEN 1993-1-14 [3] refers to prEN 1993-1-1 [10], which prescribes a basic out-of-plumb angle of ϕ_0=1/400 when cross-sections and members are checked elastically, or ϕ_0=1/200 for when cross-sections and members are verified using plastic resistances, and may be replaced by systems of equivalent horizontal forces, or the assumed shape derived from elastic buckling analyses. For member imperfections, prEN 1993-1-14 [3] recommends an imperfection amplitude of 80% of the geometric manufacturing tolerances given in EN 1090 [21], with a minimum value of L/1000, and a half-sinusoidal shape along the member length. The use of equivalent imperfections that account for the combined effect of geometric imperfections and residual stresses is also permitted. The combination of imperfections should be chosen to identify the lowest resistance; when the relevant directions are not evident, several imperfections with different directions should be investigated. Finally, cross-sectional imperfections should also be included when designing plated and cold-formed structures using advanced analysis.

The AS 4100 [4] and AS/NZS 4600 [5] Specifications for steel and cold-formed steel structures require that only the effect of frame imperfections with a basic out-of-plumb angle value of ϕ_0=1/200 be accounted for, as the effect of cross-sectional and member imperfections are already included in the elastic effective stiffnesses and member capacity calculations. However, when structures are designed using advanced analysis, frame and member imperfections should be modelled, for which a reduced out-of-plumb angle of 1/500 and a maximum value of the member imperfection equal to L/1000 are prescribed. While the advanced analysis approach is limited to compact sections in the AS 4100 [4] Specification for steel structures, and thus the modelling of cross-sectional imperfections is not necessary, the AS/NZS 4600 [5] Specification for cold-formed steel structures requires that local and distortional imperfections be included in the analysis, with the modes determined from linear buckling analyses and the scaling amplitudes given in [5]. Nevertheless, the incorporation of local and distortional imperfections is not required in advanced analysis of unbraced frames or racks.

In summary, the amplitudes assumed in the different specifications for initial out-of-plumb imperfections range between 1/500 and 1/200, while for member imperfections a consistent value of L/1000 is prescribed. These values are, however, significantly higher than the initial geometric imperfections measured from actual structures and reported in the literature. The measurements carried out on a series of multi-storey buildings [22,23] suggested that frame imperfections exhibit a mean value of 0.0013 and a standard deviation of 0.00114, which correspond to out-of-plumb angles of 1/770 and 1/877, respectively [11]. Likewise, member imperfection amplitudes reported in the literature also tend to be remarkably lower than the nominal L/1000 value prescribed in the codes, with mean values of L/1996 reported for hot-rolled steel I-section members [13] and L/3232 for cold-formed stainless steel rectangular hollow section columns [16], for example.

2.2. Initial geometric imperfections as superposition of buckling modes

The approaches for modelling initial geometric imperfections currently prescribed in international specifications are overconservative and present some additional problems, including the difficulties associated with the offset of the node coordinates when the design software does not include specific tools for the direct definition of imperfections, or the identification of the most critical combination of imperfection directions. With the aim of simplifying the definition and input of initial geometric imperfections for advanced analysis, a new procedure in which initial geometric imperfections are defined as a linear superposition of numerous buckling modes and a suitable amplitude is assigned to each of these modes was proposed by Shayan et al. [11]. Defining initial imperfections based not only on the first buckling mode, but as a combination of numerous eigenmodes, ensures that imperfections are induced in virtually all members, thereby triggering the instability associated to the actual failure mode of the structure [11,24].

Table 1
Recommended participation factors and amplitude factors to model initial geometric imperfections in steel frames using six buckling modes [11].

Type of frame	P_1	P_2	P_3	P_4	P_5	P_6	F
Braced frames	0.20	0.20	0.15	0.15	0.15	0.15	0.003
Unbraced frames	0.40	0.10	0.15	0.15	0.10	0.10	0.003

The study presented in [11] concluded that the first six modes are sufficient to accurately represent the actual shape of the initial imperfections in steel frames, and suitable imperfection amplitudes were proposed for each of the six modes. According to [11], the amplitude A_j corresponding to the buckling mode j can be determined from Eq. (3), where P_j is the normalized scale (participation) factor, F is the amplitude factor ($F = 0.003$ when six buckling modes are adopted), and H and L correspond to the total frame height and member length, respectively.

$$A_j = \begin{cases} P_j \cdot F \cdot H & \text{for sway modes} \\ P_j \cdot F \cdot L & \text{for non} - \text{sway modes} \end{cases} \quad (3)$$

The normalized participation factors P_j were calibrated based on statistical data for initial geometric imperfections obtained from the literature, considering a range of regular and irregular low-to-mid-rise frames under gravity loads, and the values summarized in Table 1 were recommended for braced and unbraced frames. While the scale factors calibrated for the different buckling modes in braced frames were very similar since all modes represented member out-of-straightness imperfections (see the P_j values in Table 1), the scale factor calibrated for the first mode in unbraced frames – which represents the out-of-plumbness of the frame – was significantly higher than those corresponding to higher modes. Since the imperfection amplitudes A_j were calibrated for a wide range of frames based on statistical data representing actual steel structures, the derived scale factors were deemed to be applicable to typical frames and have been adopted in this study to evaluate the influence of the imperfection direction on the resistance of steel frames.

3. Benchmark frames

3.1. Description of the frames

The effect of the imperfection direction on the frame resistance has been assessed for a set of different frame layouts and different materials similar to those adopted in [11,25,26]. The database comprises simple frames (see Fig. 1), the multi-storey and multi-bay frames shown in Fig. 2 and the irregular frames presented in Fig. 3, which were subjected to vertical point loads or uniformly distributed loads, including a broad range of frame geometries and boundary conditions. For each of the 20 layouts, structural steel and austenitic stainless steel materials were considered to assess whether the nonlinear stress-strain behaviour exhibited by stainless steel alloys had any influence on the effect of the imperfection direction.

The constitutive model for structural steel was assumed elastic-perfectly plastic, while to describe the nonlinear stress-strain relationship of the austenitic stainless steel alloy the two-stage Ramberg-Osgood model proposed in [27] was adopted. The material properties assumed for the structural steel and austenitic stainless steel frames are summarized in Table 2, in which E is the Young's modulus, f_y is the yield stress, f_u is the ultimate tensile strength, ε_u is the ultimate tensile strain and n and m are the nonlinear exponents for the two-stage Ramberg-Osgood model. All frames comprised compact I-section beams and columns with uniform member sizes, which were chosen from the European HEB series to produce member slenderness values of $\overline{\lambda}_c = 1.0$. The member slenderness was calculated from $\overline{\lambda}_c = \sqrt{N_{pl}/N_{cr}}$, where N_{pl} is the squash load of the cross-section and N_{cr} is the elastic buckling load. For $\overline{\lambda}_c = 1.0$, the elastic buckling load and the squash load coincide, and structures show the greatest sensitivity to initial imperfection around this slenderness value [11,28,29]. In addition, the database was extended to include additional 20 frames with HEB 340 cross-section beams and columns for the structural steel material, which resulted in member slenderness values ranging between $\overline{\lambda}_c = 0.3 - 2.4$. In total, 60 different frames were investigated.

3.2. Finite element modelling

Steel and stainless steel frames were modelled using the general-purpose finite element software ABAQUS [30] and using the 2-noded linear B31OS beam element available in the library, which is capable of accounting for the spread of plasticity through the cross-section and along the member length. Frames were restrained in the out-of-plane direction so that only in-plane major axis bending/buckling was considered. The ultimate load factors for each frame, which are the load factors corresponding to the ultimate load or resistance of the frames, were determined from second-order inelastic analyses that accounted for all material and geometric nonlinearities (advanced analysis) using the Riks arc-length technique available in ABAQUS [30].

Beam-to-column connections were assumed to be rigid, and loads were introduced in the beams or at the beam-to-column joints using

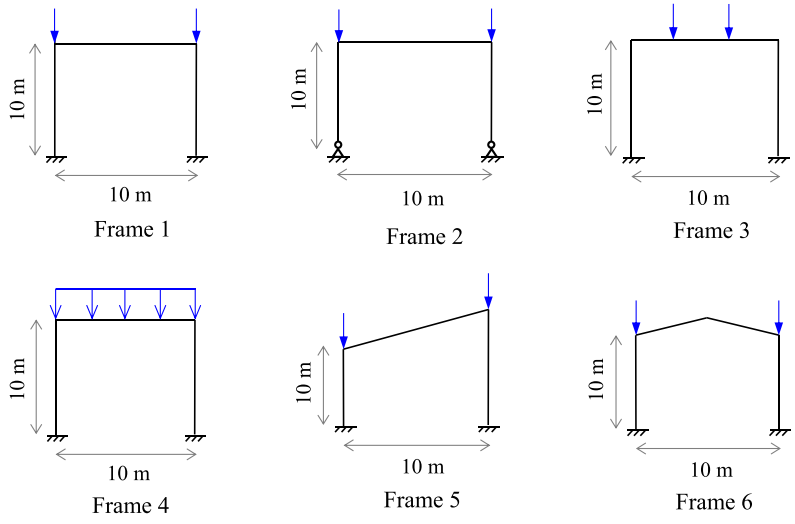

Fig. 1. Simple frame layouts considered in the study (adapted from [25,26]).

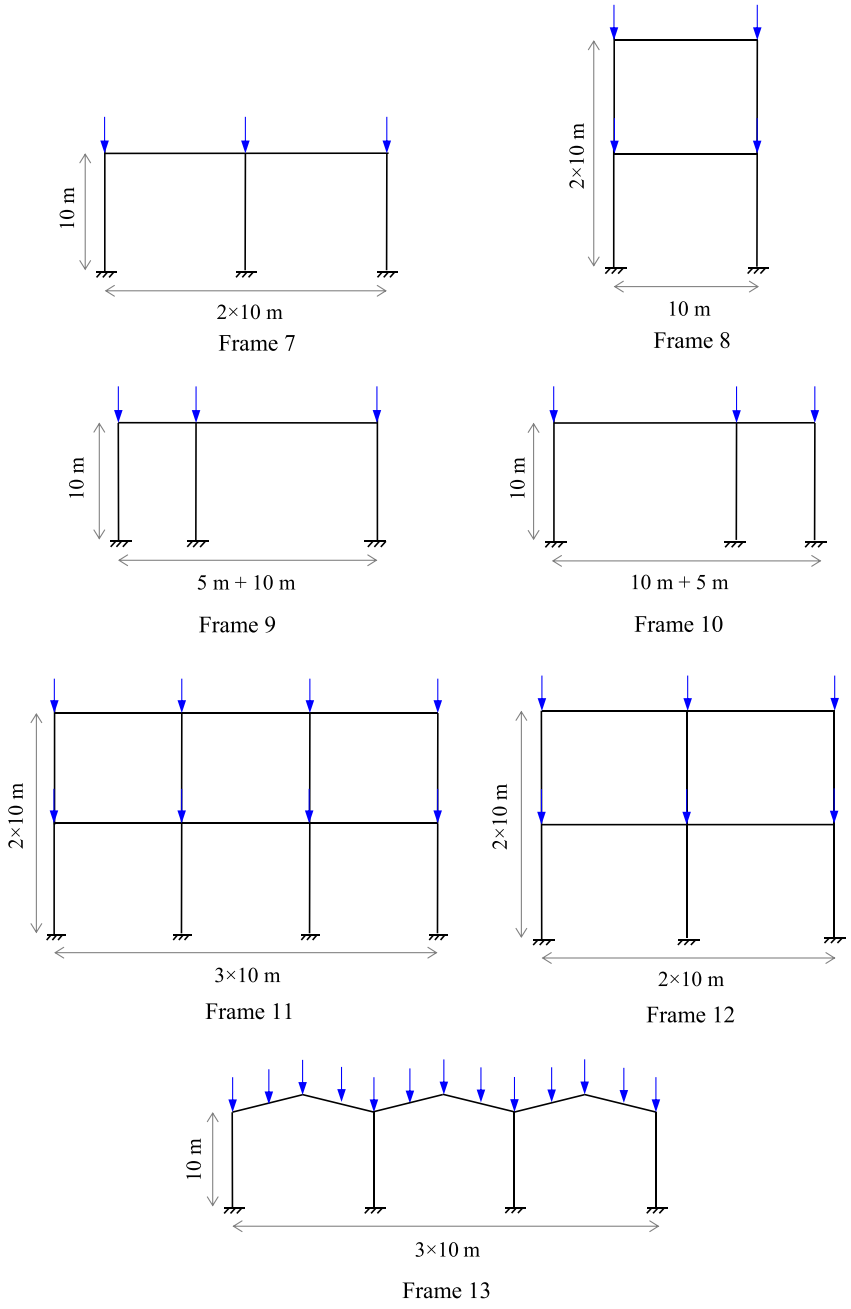

Fig. 2. Multi-storey and multi-bay frame layouts considered in the study (adapted from [25,26]).

distributed or point loads, as indicated in Figs. 1-3. The base supports of most of the frames were assumed as fixed, although frames with pin-ended boundary conditions were also investigated (i.e., Frames 2 and 15). Material properties were introduced as user-defined true stress-plastic strain relationships using the elastic-perfectly plastic or nonlinear [27] material models for structural steel and stainless steel, respectively. In order to investigate the influence of imperfection direction only on the ultimate frame resistances, residual stresses were not taken into account in this study, following the approach adopted in [11].

Initial geometric imperfections were introduced as a superposition of the first six buckling modes using the *IMPERFECTION option in ABAQUS, which were obtained from a priori elastic buckling analysis, and the amplitudes of each mode were determined from the scaling factors proposed in [11] and described in Section 2.2. All possible combinations of imperfection directions were investigated by assigning a positive (+1) or negative (−1) sign to each of these amplitudes and by combining them using the MESH combination option available in ABAQUS [30], which resulted in $2^6 = 64$ different analyses for each of the investigated frames. The MESH combination pattern in ABAQUS combines every sampled value of a parameter with every sampled value of every other parameter in the parametric study [30]; considering that the sampled parameters in this study were the signs of the six imperfection shapes determined from the elastic buckling analyses (parameters adopted the values [−1,+1]), this procedure guaranteed that the two possible directions (i.e, signs) of each mode were combined with all the possible directions of the other five imperfection shapes. In total, 3840 advanced analyses were performed on steel and stainless steel frames. Fig. 4 shows three examples of imperfection direction combinations for Frame 1: the

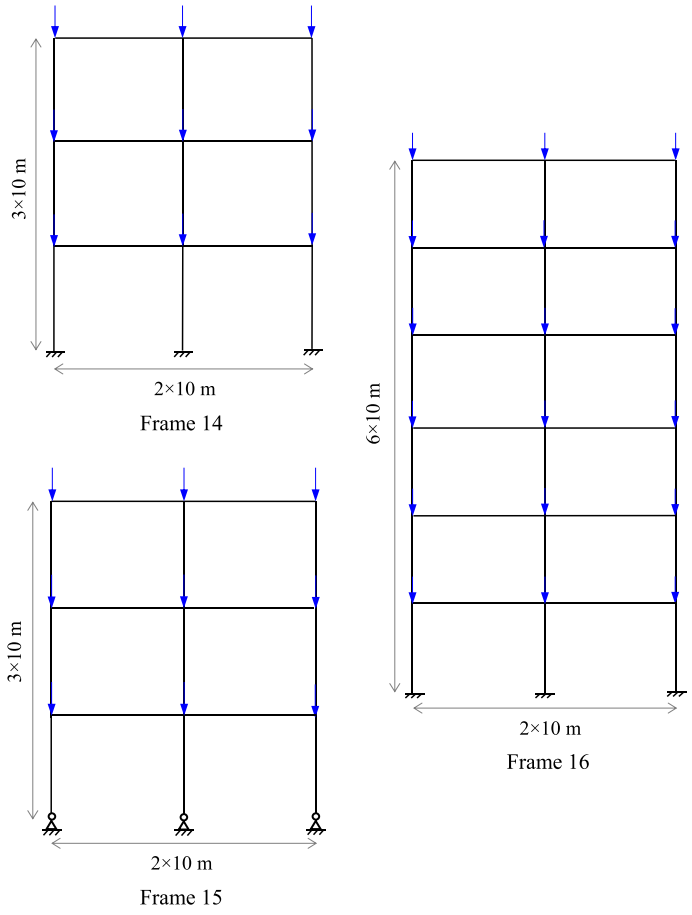

Fig. 2. (*continued*).

initial imperfection pattern corresponding to the linear superposition of six buckling modes with all positive (red) and all negative (blue) amplitudes are shown, in addition to an intermediate case with a combination of positive and negative directions (green). The initial geometry of the perfect frame is also shown as reference.

4. Influence of the imperfection direction on the frame resistance

4.1. Illustrative example

To illustrate the influence of the initial imperfection introduced in finite element models, a simple pitched portal frame subjected to two point loads at the beam-to-column joints (see Frame 6 in Fig. 1) was investigated. Several advanced analyses with different initial geometric imperfections were carried out, and the failure modes and frame resistances were compared. Imperfection patterns including global sway imperfections and member imperfections were obtained from an elastic buckling analysis, and combined using different amplitudes. Fig. 5 shows the failure modes and ultimate loads (taken as the maximum loads of the load-displacement curves and which represent the resistance of the frames) obtained for Frame 6 considering different types, combinations and amplitudes of sway and member imperfections. When combinations of sway and member imperfections were considered following the requirements in international steel standards, using amplitudes of ϕ=1/200 and e_0=L/1000, respectively, the advanced simulations predicted sway-type failure modes and the same ultimate loads for the four possible combinations of frame and member imperfection directions (see Fig. 5(a)), which indicated a negligible effect of the imperfection directions on the ultimate response of the frame.

On the contrary, when only member imperfections following the non-sway buckling modes and amplitudes e_0 of the member imperfection equal to L/1000 and L/200 were introduced, a clear dependency on the imperfection direction was observed for the two amplitudes of member imperfection. The failure modes and ultimate loads reported in Fig. 5(c)-(f) highlight the influence and importance of the initial imperfection pattern considered in advanced analysis, as the choice of some imperfection combinations led to failure modes similar to those obtained when global sway imperfections were introduced (cases (c) and (f), when the imperfections of both columns lean in the same direction), while other combinations resulted in significantly higher ultimate load predictions when they locked in failure modes with higher critical loads (as per cases (d) and (e)). The values of the ultimate loads were different for the two member imperfection amplitudes considered (i.e., L/1000 and L/200), as shown in Fig. 5, but the conclusions are the same. The analysis also showed that even for very small initial sway imperfection amplitudes (i.e., ϕ=1/5000, significantly smaller that the 1/200 or 1/500 values specified in the codes), the frame exhibited sway-type failure modes for the four combinations of member imperfection directions (as per in Fig. 5(b)), although resulted in higher ultimate loads than the F_u=282 kN value predicted using the sway imperfection amplitude prescribed in the codes (case (a)). This highlighted the influence out-of-plumbness imperfections had not only on the ultimate load of the frame, but also on the failure mode observed. In a similar way, the fact that small sway imperfections were sufficient to result in sway failure modes emphasizes the importance of introducing a combination of different buckling modes as initial imperfections when designing frames using advanced analysis (especially sway

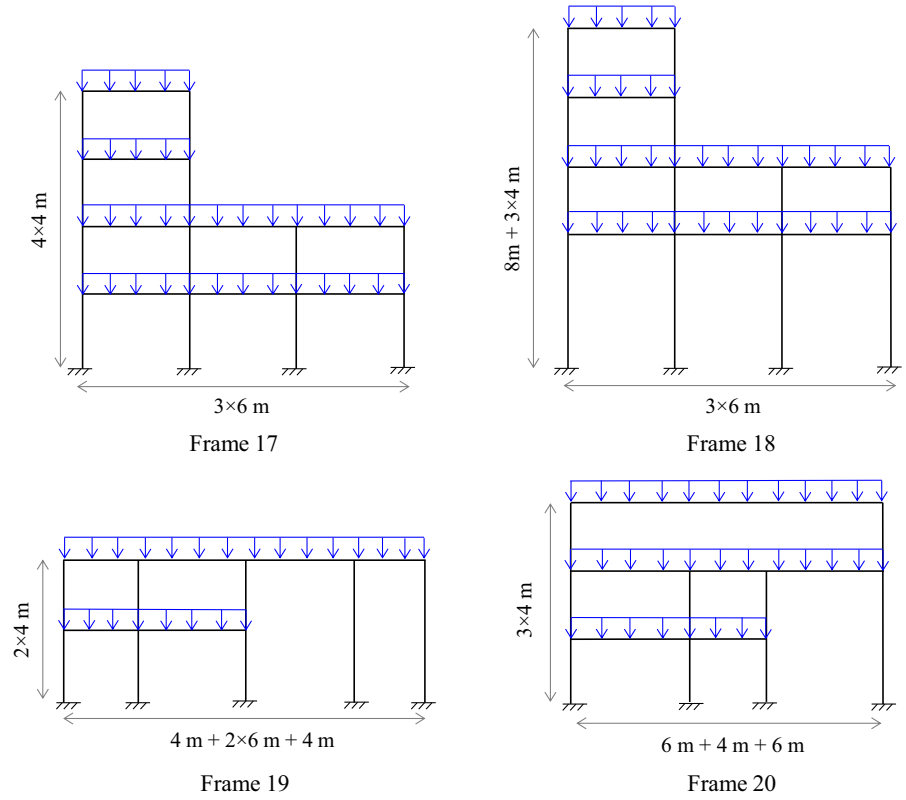

Fig. 3. Irregular frame layouts considered in the study (adapted from [11]).

Table 2
Material properties for structural steel and austenitic stainless steel frames.

Alloy	E [GPa]	f_y [MPa]	f_u [MPa]	ε_u [mm/mm]	n [−]	m [−]
Structural steel	210	235	–	–	–	–
Austenitic stainless steel	200	310	670	0.54	6.3	2.6

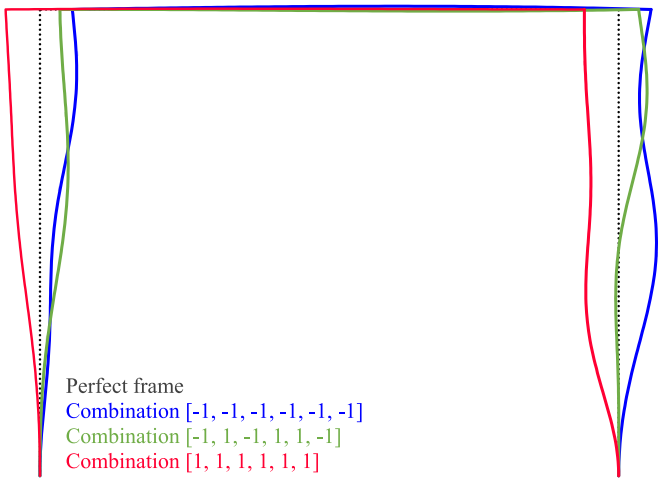

Fig. 4. Initial geometric imperfection patterns resulting from the linear combination of six buckling modes with different directions (amplitude signs).

imperfections), to ensure that the critical shape is present and that the instability associated with the actual failure mode of the structure is triggered [11,24].

4.2. Influence of the initial imperfection direction

The influence of the imperfection direction on the frame resistance is assessed in this Section based on the finite element analyses of steel and stainless steel frames presented in Section 3. Advanced finite element analyses (i.e., GMNIA analyses) were carried out for each of the frame layouts, cross-sections and materials investigated, in which initial geometric imperfections were introduced as the linear superposition of the first six buckling modes using the amplitudes recommended in [11] and introduced in Section 2.2. The study considered all possible combinations of imperfection directions for the six buckling modes, obtaining 64 different ultimate load factors λ_u for each frame investigated, and the variability of these load factors was evaluated.

The assessment of the ultimate load factors λ_u is presented in Tables 3-5. While Table 3 presents the results for steel frames with multiple column slenderness $\overline{\lambda}_c$ values (constant HEB 340 cross-section assumed for all columns and beams), Tables 4 and 5 report the results for steel and stainless steel frames with column slenderness values of $\overline{\lambda}_c = 1.0$, respectively. In these tables, the maximum-to-minimum ultimate load factor ratios $\lambda_{u,max}/\lambda_{u,min}$ and the coefficients of variation (COV) of the ultimate load factors are reported for each frame considered. The $\lambda_{u,max}$ load factor corresponds to the maximum of the 64 ultimate load factor values predicted for each frame, while $\lambda_{u,min}$ is the minimum of the 64 ultimate load factor values, which according to the draft European guidelines [3] corresponds to the most critical combination of initial imperfections and should be adopted as the nominal imperfection when designing with advanced analysis. Tables 3-5 also report the $\lambda_{u,pos}/\lambda_{u,min}$ ratios, where $\lambda_{u,pos}$ is the ultimate load factor for the imperfection combination that assumes all positive amplitudes, and the percentage of ultimate load factors below $\lambda_{u,pos}$ for each frame. Note that when determining the imperfection shape assuming all positive amplitudes, the mode shapes are taken as produced by the buckling analysis, and so are arbitrarily assigned a sign, i.e., the direction of the individual buckling mode is arbitrary.

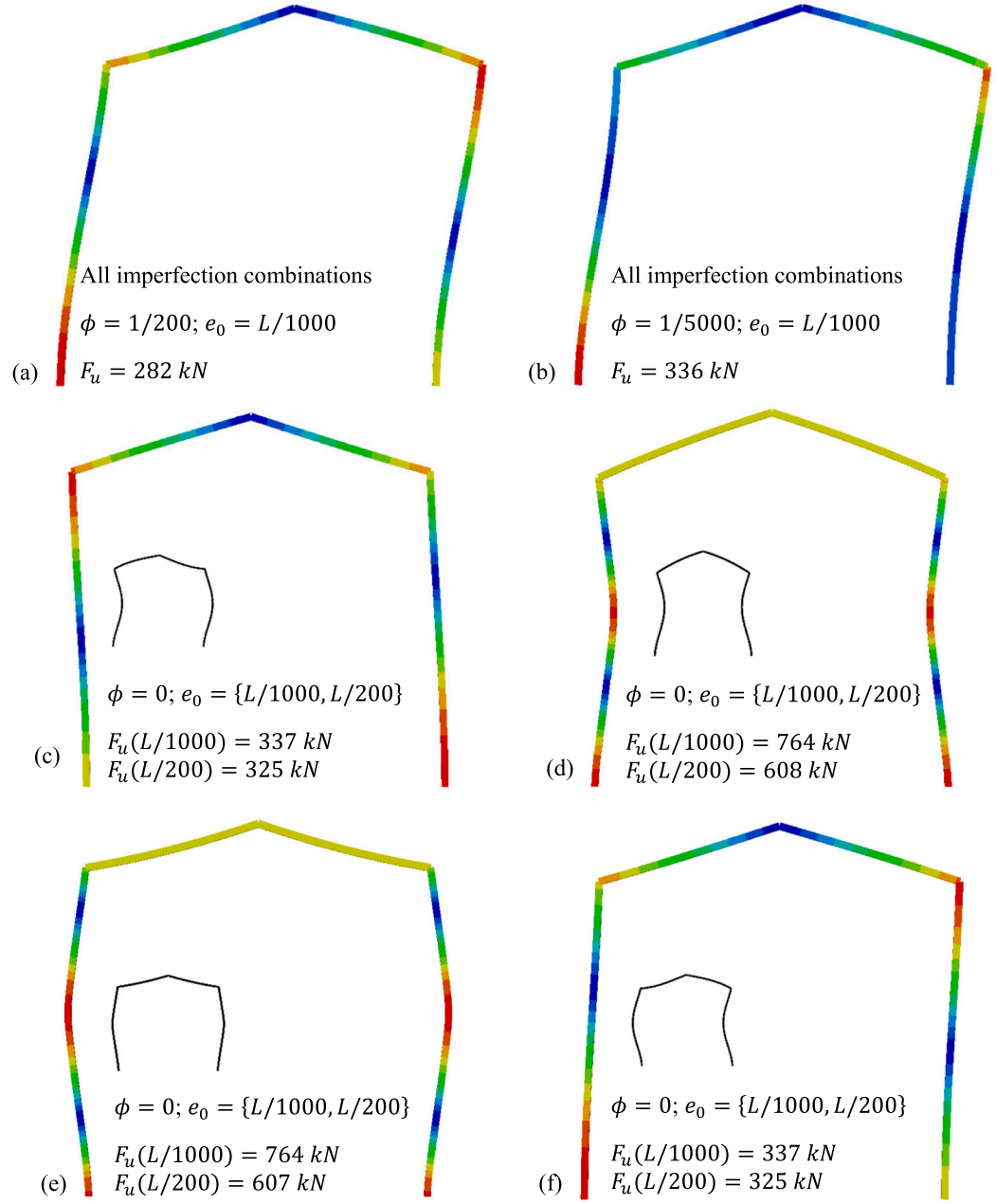

Fig. 5. Illustrative example: failure modes and ultimate loads for Frame 6 considering different types, combinations and amplitudes of sway and member imperfections; imperfection shown in black insert in (c-f).

The results shown in Tables 3–5 suggest that the influence of the imperfection direction on the predicted ultimate frame load is small. The differences between the maximum and minimum load factors within each frame lie between 0 and 6%, and very low coefficients of variation are observed (0.00–0.03). Given that the normalized scale factors P_i reported in Table 1 for buckling modes 2 to 6 representing the out-of-straightness of members are significantly lower than the P_1 factor for the out-of-plumbness of unbraced frames, these results suggest that the influence of the highest buckling modes on the ultimate load of the investigated frames is low. This is in line with the sensitivity analysis results reported in [28], which indicated that the influence of the initial sway imperfections on the resistance of steel frames is much more significant than that of initial member imperfections. The results also show that the variability in the ultimate load factors is not significantly affected by the material or the type of frame, since the $\lambda_{u,max}/\lambda_{u,min}$ ratios and COV values reported in Tables 3–5 are very similar for steel and stainless steel frames, and for simple, multi-storey, multi-bay and irregular frames.

The $\lambda_{u,pos}/\lambda_{u,min}$ ratios reported in these tables also indicate that while, in general, the ultimate load factors corresponding to the critical imperfection combination $\lambda_{u,min}$ of course are lower than the ultimate load factors for the imperfection combination with all positive amplitudes $\lambda_{u,pos}$, the differences observed are insignificant, with all $\lambda_{u,pos}/\lambda_{u,min}$ ratios ranging between 1.00 and 1.01 in Tables 3-5. The number of imperfection direction combination cases in which the ultimate load factor is lower than $\lambda_{u,pos}$ depends on the frame, but ranges between 0 and 58%. The same results are illustrated in Fig. 6, in which the $\lambda_{u,max}/\lambda_{u,min}$ and $\lambda_{u,pos}/\lambda_{u,min}$ ratios are presented for the different steel and stainless steel frames investigated as functions of the member slenderness of the critical column $\overline{\lambda}_c$. These results indicate that the maximum variability in ultimate load factors (i.e., highest $\lambda_{u,max}/\lambda_{u,min}$ ratios) generally occurs for frames with member slenderness values $\overline{\lambda}_c$ of around

Table 3
Ultimate load factor assessment for steel frames with HEB 340 cross-section (multiple column slenderness $\bar{\lambda}_c$ values).

Frame	$\lambda_{u,max}/\lambda_{u,min}$	COV	$\lambda_{u,pos}/\lambda_{u,min}$	Cases below $\lambda_{u,pos}$ [%]
Frame 1	1.040	0.013	1.000	0.0
Frame 2	1.027	0.012	1.002	37.5
Frame 3	1.003	0.000	1.003	6.3
Frame 4	1.002	0.001	1.002	31.3
Frame 5	1.039	0.010	1.010	1.6
Frame 6	1.029	0.011	1.000	0.0
Frame 7	1.025	0.011	1.004	25.0
Frame 8	1.045	0.015	1.003	9.4
Frame 9	1.032	0.015	1.000	0.0
Frame 10	1.029	0.014	1.000	0.0
Frame 11	1.009	0.002	1.009	3.1
Frame 12	1.020	0.007	1.000	0.0
Frame 13	1.005	0.002	1.002	48.4
Frame 14	1.026	0.010	1.004	25.0
Frame 15	1.033	0.016	1.002	37.5
Frame 16	1.023	0.008	1.006	32.8
Frame 17	1.024	0.011	1.002	31.3
Frame 18	1.051	0.025	1.000	0.0
Frame 19	1.001	0.000	1.001	3.1
Frame 20	1.008	0.004	1.008	50.0

Table 4
Ultimate load factor assessment for steel frames with column slenderness $\bar{\lambda}_c = 1.0$.

Frame	$\lambda_{u,max}/\lambda_{u,min}$	COV	$\lambda_{u,pos}/\lambda_{u,min}$	Cases below $\lambda_{u,pos}$ [%]
Frame 1	1.041	0.014	1.001	1.6
Frame 2	1.036	0.014	1.006	26.6
Frame 3	1.002	0.001	1.002	57.8
Frame 4	1.010	0.005	1.000	0.0
Frame 5	1.040	0.013	1.004	9.4
Frame 6	1.038	0.013	1.000	0.0
Frame 7	1.031	0.011	1.004	26.6
Frame 8	1.037	0.015	1.004	15.6
Frame 9	1.035	0.013	1.000	0.0
Frame 10	1.030	0.015	1.000	0.0
Frame 11	1.010	0.003	1.010	12.5
Frame 12	1.015	0.007	1.001	1.6
Frame 13	1.010	0.005	1.000	0.0
Frame 14	1.024	0.011	1.003	25.0
Frame 15	1.040	0.019	1.000	0.0
Frame 16	1.026	0.008	1.006	31.3
Frame 17	1.012	0.005	1.001	3.1
Frame 18	1.055	0.026	1.000	0.0
Frame 19	1.003	0.000	1.002	9.4
Frame 20	1.020	0.004	1.010	15.6

1.0, while the influence of $\bar{\lambda}_c$ on the $\lambda_{u,pos}/\lambda_{u,min}$ ratios is less remarkable.

Overall, the assessment of the ultimate load factors presented in this Section highlights the fact that the adoption of a linear combination of buckling modes that assumes all modes with positive amplitudes ($\lambda_{u,pos}$) is a simple approach that estimates the minimum ultimate load ($\lambda_{u,min}$) with good accuracy, without requiring that all possible combinations be considered to find the critical imperfection combination, as required by prEN 1993-1-14 [3]. Provided sufficient imperfection types are introduced through the consideration of different sway and non-sway modes, designers can simply adopt initial geometric imperfections resulting from the approach proposed in [11], with all positive amplitudes, and obtain a sufficiently accurate prediction of the ultimate frame load. Fig. 7 shows the histogram for all the ultimate load factors λ_u normalized by the corresponding $\lambda_{u,pos}$ factor for all the frames considered in the analysis. Fig. 7 clearly shows that the great majority of the $\lambda_u/\lambda_{u,pos}$ ratios lie in the 0.99–1.02 range, with the mean and standard deviation of $\lambda_u/\lambda_{u,pos}$ being 1.009 and 0.014, respectively.

It should be noted that the total imperfection amplitudes resulting from the mode scale factors proposed in [11] are sometimes significantly lower than those prescribed in the different specifications, as discussed in Section 2.1. To evaluate the actual imperfection amplitudes introduced in the finite element models by means of the linear superposition of the six buckling modes, sway and member imperfections were back-calculated from the developed ABAQUS models using the initial node coordinates. Out-of-plumb angles were estimated from the relative displacements of the bottom and top ends of the columns, while member imperfections were calculated as the differences between the total imperfections and the imperfections corresponding to the out-of-plumbness for each node. From these results, out-of-plumb angles determined from the participation and amplitude factors reported in Table 1 were found to lie between 1/260 and 1/1080 for the frames analysed, while the resulting member imperfection amplitudes ranged between L/825 and L/8440, depending on the column considered. In order to evaluate whether the conclusions drawn in this Section are still valid for frames with larger initial imperfections, similar to those prescribed in the codes, the influence of the imperfection amplitude on the variability of ultimate load factors is investigated in the next Section.

Table 5
Ultimate load factor assessment for austenitic stainless steel frames with column slenderness $\bar{\lambda}_c = 1.0$.

Frame	$\lambda_{u,max}/\lambda_{u,min}$	COV	$\lambda_{u,pos}/\lambda_{u,min}$	Cases below $\lambda_{u,pos}$ [%]
Frame 1	1.032	0.013	1.000	0.0
Frame 2	1.033	0.011	1.002	21.9
Frame 3	1.003	0.001	1.001	12.5
Frame 4	1.011	0.005	1.001	4.7
Frame 5	1.030	0.011	1.010	10.9
Frame 6	1.030	0.011	1.000	0.0
Frame 7	1.051	0.024	1.000	0.0
Frame 8	1.032	0.015	1.002	21.9
Frame 9	1.022	0.010	1.000	0.0
Frame 10	1.030	0.015	1.000	0.0
Frame 11	1.000	0.000	1.000	0.0
Frame 12	1.012	0.006	1.001	21.9
Frame 13	1.000	0.000	1.000	0.0
Frame 14	1.030	0.008	1.010	7.8
Frame 15	1.034	0.015	1.002	25.0
Frame 16	1.012	0.005	1.001	14.1
Frame 17	1.023	0.011	1.000	0.0
Frame 18	1.060	0.025	1.000	0.0
Frame 19	1.023	0.009	1.000	0.0
Frame 20	1.001	0.001	1.001	34.4

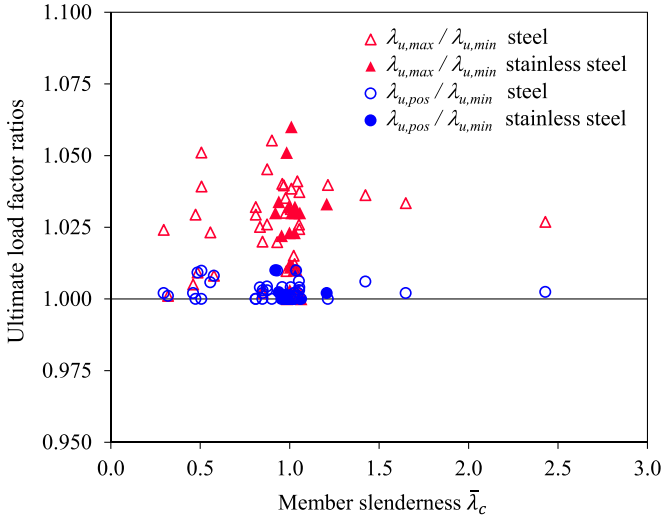

Fig. 6. Assessment of the influence of the imperfection direction on the ultimate load factors λ_u for steel and stainless steel frames.

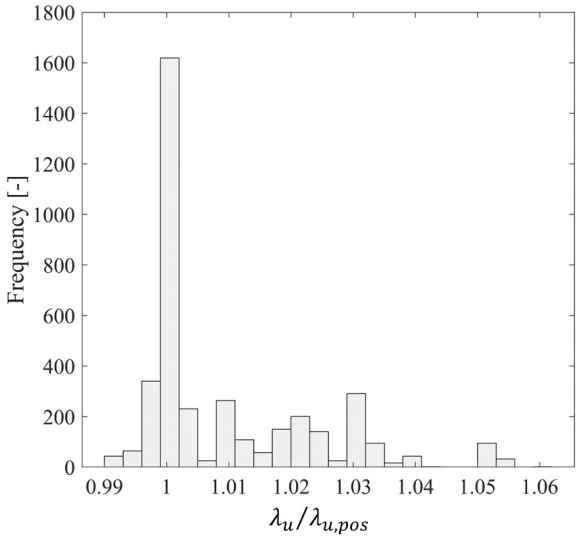

Fig. 7. Histogram for the $\lambda_u/\lambda_{u,pos}$ ultimate load factor ratios for steel and stainless steel frames.

Table 6
Ultimate load factor assessment for steel frames with column slenderness λ_c = 1.0 and double imperfection amplitude.

Frame	$\lambda_{u,max}/\lambda_{u,min}$	COV	$\lambda_{u,pos}/\lambda_{u,min}$	Cases below $\lambda_{u,pos}$ [%]
Frame 1	1.057	0.025	1.000	0.0
Frame 12	1.032	0.012	1.002	9.4
Frame 17	1.031	0.014	1.000	0.0
Frame 20	1.020	0.007	1.010	21.9

4.3. Influence of the initial imperfection amplitude

As indicated above, the imperfection amplitudes resulting from the combination of the different buckling modes using the scaling parameters proposed in [11] are considerably lower than the values typically prescribed in design provisions for sway and member imperfections for some of the investigated frames, since the amplitude factor F was calibrated using data on actual initial imperfection measurements. With the objective of assessing the influence of the initial imperfection amplitude on the variability of the frame resistance, and whether the conclusions drawn in Section 4.2 are still valid for higher imperfection amplitudes, more similar to those specified in the codes, the analysis presented in the previous Section was repeated for four of the frames investigated (Frame 1, Frame 12, Frame 17 and Frame 20) assuming imperfection amplitudes equal to two times the values proposed in [11] (i.e., adopting F=0.006 in Eq. (3)). The imperfections resulting from this assumption lie between out-of-plumb angles of 1/130 and 1/540 and member imperfection amplitudes between L/413 and L/4220, and thus constitute an upper limit to the initial imperfection magnitudes prescribed in the codes.

Results were obtained for steel frames with member slenderness values of $\bar{\lambda}_c$ = 1.0, since the analysis presented in Section 4.2 showed that while there is very little influence of the material type, the maximum deviations in ultimate load factors occur for $\bar{\lambda}_c$ = 1.0. The $\lambda_{u,max}/\lambda_{u,min}$ and $\lambda_{u,pos}/\lambda_{u,min}$ ratios corresponding to the new analysis are reported in Table 6, where the coefficients of variation of the ultimate load factors and the cases with $\lambda_u < \lambda_{u,pos}$ are also included. Comparing the results in Table 6 with the equivalent values reported in Table 4, it can be seen that the $\lambda_{u,max}/\lambda_{u,min}$ ratios and COV values increase for higher imperfection amplitudes, as does the number of cases with ultimate load factors below $\lambda_{u,pos}$. However, the $\lambda_{u,pos}/\lambda_{u,min}$ ratios remain practically unchanged. This indicates that although the variability of the load factors is slightly higher, the adoption of initial geometric imperfections resulting from the superposition of buckling modes with all positive directions is still acceptable for imperfection amplitudes similar to those prescribed in the different specifications. As the $\lambda_{u,pos}/\lambda_{u,min}$ ratios observed for F=0.003 and F=0.006 were similar, it is inferred that the results for the amplitudes prescribed in specifications will lie within the two scenarios investigated.

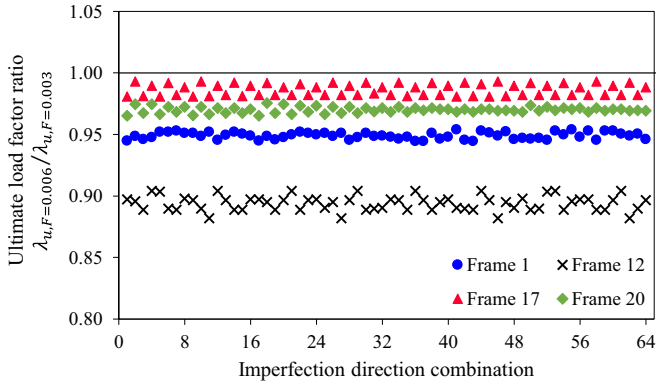

Fig. 8. Influence of the initial imperfection amplitude on the frame resistance.

Finally, Fig. 8 compares the ultimate load factors obtained for the original amplitude factor F=0.003 proposed in [11] with those corresponding to the double imperfection amplitudes investigated in this Section for the four frames analysed. The ratios between the ultimate load factors λ_u corresponding to F=0.006 and F=0.003 (i.e., $\lambda_{u,F=0.006}/\lambda_{u,F=0.003}$) were calculated for the same imperfection direction combinations, and plotted for Frame 1, Frame 12, Frame 17 and Frame 20 to evaluate the influence of the initial imperfection amplitudes on the frame resistance. The ratios reported in Fig. 8 indicated that, as expected, the $\lambda_{u,F=0.006}/\lambda_{u,F=0.003}$ ratios lie below unity for all the frames investigated in this Section because the ultimate load factors corresponding to the larger imperfection amplitudes $\lambda_{u,F=0.006}$ were lower. Fig. 8 also shows that the different frames exhibited a distinct sensitivity to the initial imperfection magnitude, with Frame 12 being the most sensitive among the frames analysed, with a difference in ultimate loads of around 10%, followed by Frame 1, with a 5% difference, and Frames 20 and 17, with differences of 3% and 1%, respectively. The results also showed that the influence of the initial imperfection amplitude on the ultimate loads was quite uniform for the different imperfection direction combinations, which ultimately results in similar levels of ultimate load factor variability for the two imperfection amplitude levels, F=0.003 and F=0.006, as discussed above.

5. Conclusions

Initial imperfections present in steel structures include global (frame) sway imperfections, member out-of-straightness imperfections and cross-sectional (local or distortional) imperfections. The nonlinear response of structures can be considerably influenced by initial geometric imperfections, and both the stiffness and the resistance can be affected. Hence, initial imperfections need to be modelled in advanced structural finite element models. Based on the method proposed by Shayan et al. [11] to model initial geometric imperfections as a linear combination of the first six buckling modes, this paper investigates the influence of the imperfection direction on the ultimate response of steel and stainless steel frames in advanced analysis. The study is based on a set of simple, multi-storey, multi-bay and irregular unbraced frames, featuring structural steel and austenitic stainless steel alloys and a range of member slenderness values, for which the ultimate load factors corresponding to all the different possible combinations of imperfection directions were determined and analysed. The assessment of the ultimate load factors showed that the influence of the imperfection direction on the ultimate load is small for the investigated frames, and no

significant differences were observed for simple, multi-storey, multi-bay or irregular frames or for different materials. The results also indicated that the adoption of a linear combination of buckling modes that assumes all six modes with positive amplitudes is a simple yet congruous approach to modelling geometric imperfections. For codes that require the geometric imperfection to be chosen as the worst case scenario, the approach provides resistances close to the minimum frame resistance.

Author statement

Itsaso Arrayago: Finite Element model development and simulations, Data curation, Methodology, Formal analysis, Writing - Original Draft.

Kim J.R. Rasmussen: Methodology, Supervision, Writing - Review & Editing.

Declaration of Competing Interest

The authors declare that they have no known competing financial interests or personal relationships that could have appeared to influence the work reported in this paper.

Acknowledgements

The project leading to this research has received funding from the European Union's Horizon 2020 Research and Innovation Programme under the Marie Sklodowska-Curie Grant Agreement No. 842395.

References

[1] American Institute of Steel Construction (ANSI/AISC), AISC 360. Specification for Structural Steel Buildings. Illinois, USA, 2016.
[2] American Institute of Steel Construction (ANSI/AISC), AISC 370. Specification for Structural Stainless Steel Buildings. Illinois, USA, 2021.
[3] Working Group 22 for Eurocode 3 CEN/TC 250/SC3/WG22, prEN 1993-1-14. Eurocode 3: Design of Steel Structures – Part 1–14: Design Assisted by Finite Element Analysis. Final Document. Brussels, Belgium, 2021.
[4] AS 4100 Steel Structures, Standards Australia, Sydney, Australia, 2020.
[5] AS/NZS 4600 Cold-formed Structures, Standards Australia, Sydney, Australia, 2018.
[6] S.L. Chan, H.Y. Huang, L.X. Fang, Advanced analysis of imperfect portal frames with semirigid base connections, J. Eng. Mech. (ASCE) 131 (6) (2005) 633–640.
[7] S.E. Kim, Practical Advanced Analysis for Steel Frame Design, Ph.D. Thesis, Purdue University, West Lafayette, IN, 1996.
[8] M. Kucukler, L. Gardner, L. Macorini, A stiffness reduction method for the in-plane design of structural steel elements, Eng. Struct. 73 (2014) 72–84.
[9] I. González-de-León, I. Arrayago, E. Real, E. Mirambell, A stiffness reduction method for the in-plane design of stainless steel members and frames according to EN 1993-1-4, Eng. Struct. 253 (2022) 113740, https://doi.org/10.1016/j.engstruct.2021.113740.
[10] European Committee for Standardization (CEN), prEN 1993-1-1. Eurocode 3: Design of Steel Structures – Part 1–1: General Rules and Rules for Buildings. Final Document. Brussels, Belgium, 2019.
[11] S. Shayan, K.J.R. Rasmussen, H. Zhang, On the modelling of initial geometric imperfections of steel frames in advanced analysis, J. Constr. Steel Res. 98 (2014) 167–177.
[12] R. Bjorhovde, Deterministic and Probabilistic Approaches to the Strength of Steel Columns, PhD dissertation, Lehigh University, Bethlehem, Pa, 1972.
[13] Y. Fukumoto, Y. Itoh, Evaluation of multiple column curves using the experimental data-base approach, J. Constr. Steel Res. 3 (3) (1983) 2–19.
[14] H. Zhang, H. Liu, B.R. Ellingwood, K.J.R. Rasmussen, System reliabilities of planar gravity steel frames designed by the inelastic method in AISC 360-10, J. Struct. Eng. ASCE 144 (3) (2018) 04018011.
[15] K.J.R. Rasmussen, H. Zhang, Future challenges and developments in the design of steel structures – an Australian perspective, in: Proceedings of the 8th European Conference on Steel and Composite Structures (EUROSTEEL 2017). Copenhagen, Denmark, 2017.
[16] I. Arrayago, K.J.R. Rasmussen, E. Real, Statistical analysis of the material, geometrical and imperfection characteristics of structural stainless steels and members, J. Constr. Steel Res. 175 (2020), 106378.
[17] F.S. Cardoso, H. Zhang, K.J.R. Rasmussen, S. Yan, Reliability calibrations for the design of cold-formed steel portal frames by advanced analysis, Eng. Struct. 182 (2019) 164–171.
[18] W. Liu, H. Zhang, K.J.R. Rasmussen, System reliability-based direct design method for space frames with cold-formed steel hollow sections, Eng. Struct. 166 (2018) 79–92.
[19] I. Arrayago, K.J.R. Rasmussen, System-based reliability analysis of stainless steel frames under gravity loads, Eng. Struct. 231 (2021), 111775.
[20] W. Liu, H. Zhang, K.J.R. Rasmussen, S. Yan, System-based limit state design criterion for 3D steel frames under wind loads, J. Constr. Steel Res. 157 (2019) 440–449.
[21] European Committee for Standardization (CEN), EN 1090–2. Execution of Steel Structures and Aluminium Structures. Technical Requirements for Steel Structures. Brussels, Belgium, 2018.
[22] D. Beaulieu, P.F. Adams, The results of a survey on structural out-of-plumbs, Can. J. Civ. Eng. 5 (4) (1978) 462–470.
[23] J. Lindner, R. Gietzelt, Assumptions for imperfections for out-of-plumb of columns, Stahlbau 53 (4) (1984) 97–102.
[24] K.J.R. Rasmussen, G.J. Hancock, Geometric imperfections in plated structures subject to interaction between buckling modes, Thin-Walled Struct. 6 (1988) 433–452.
[25] F. Walport, L. Gardner, D.A. Nethercot, A method for the treatment of second order effects in plastically-designed steel frames, Eng. Struct. 200 (2019), 109516.
[26] F. Walport, I. Arrayago, L. Gardner, D.A. Nethercot, Assessment and treatment of second order effects in plastically-designed stainless steel frames, J. Constr. Steel Res. 187 (2021), 106981.
[27] I. Arrayago, E. Real, L. Gardner, Description of stress–strain curves for stainless steel alloys, Mater. Des. 87 (2015) 540–552.
[28] Z. Kala, Sensitivity analysis of steel plane frames with initial imperfections, Eng. Struct. 33 (8) (2011) 2342–2349.
[29] M.J. Clarke, R.Q. Bridge, G.J. Hancock, N.S. Trahair, Advanced analysis of steel building frames, J. Constr. Steel Res. 23 (1–3) (1992) 1–29.
[30] ABAQUS, Version 6.10. Simulia, Dassault Systèmes, France, 2010.